Two-stage risk-constrained stochastic optimal bidding strategy of virtual power plant considering distributed generation outage

Ghasemi-Olanlari, Farzin; Moradi-Sepahvand, Mojtaba; Amraee, Turaj

DOI
10.1049/gtd2.12826

Publication date
2023

Document Version
Final published version

Published in
IET Generation, Transmission and Distribution

Received: 22 December 2022 | Revised: 14 February 2023 | Accepted: 10 March 2023

IET Generation, Transmission & Distribution

DOI: 10.1049/gtd2.12826

The Institution of Engineering and Technology WILEY

ORIGINAL RESEARCH

Two-stage risk-constrained stochastic optimal bidding strategy of virtual power plant considering distributed generation outage

Farzin Ghasemi-Olanlari[1] | Mojtaba Moradi-Sepahvand[2] | Turaj Amraee[1]

[1]Electrical Engineering Faculty, K. N. Toosi University of Technology, Tehran, Iran

[2]Department of Electrical Sustainable Energy, Delft University of Technology, Delft, The Netherlands

Correspondence
Turaj Amraee, Electrical Engineering Faculty, K. N. Toosi University of Technology, Tehran, Iran.
Email: amraee@kntu.ac.ir

Abstract

This paper presents an optimal bidding strategy for a technical and commercial virtual power plant (VPP) in medium-term time horizon. A VPP includes various distributed energy resources (DERs) that can participate in the Pool and Futures markets. Although medium/long-term scheduling provides the opportunity to participate in the futures market, it also raises the possibility of unit failure. In this regard, the impact of distributed generation (DG) units' failure, as an important challenge in VPP, is incorporated in the proposed model. The model is formulated as a risk-constrained two-stage stochastic problem. The VPP signs futures market contracts in the first stage, and in the second stage, it participates in the day-ahead (DA) market and manages its DERs. Long short-term memory neural network and scenario generation and reduction methods are used to capture the uncertainty parameters of electrical load, DA market prices, wind speed, and solar radiation in the proposed model. The performance of proposed model is investigated in different cases. The obtained results show that the VPP can compensate the losses caused by the DG units' failure through taking advantage of the arbitrage opportunity.

1 | INTRODUCTION

1.1 | Motivation

The restructuring and liberalization of the power system provide various economic opportunities for electricity producers in the electricity markets. In this regard, the producers can sell their electrical power in a competitive environment [1]. In the wholesale electricity market, the participants were mainly large and medium-sized producers, and small producers could not enter this competitive environment due to their insignificant capacity. In recent years, the penetration of distributed energy resources (DERs), which includes distributed generation (DG), energy storage systems (ESS), renewable energy systems (RES) and flexible loads (FL), is increased, and this trend is expected to grow in the coming years [2]. DERs can not only supply the growing electrical load of the distribution network, but they can also reduce power transmission costs and fossil fuel costs. Additionally, since these units produce less pollution than conventional power plants, greenhouse gas emissions are decreased [3]. Despite these advantages, DERs are still considered small-scale resources and are unable to compete with other wholesale electricity market participants. So, they must be aggregated and managed as a single entity to overcome this challenge. Two of the most common concepts of aggregating DERs are micro-grids and VPPs, which are discussed in detail in [4].

VPP is a concept that uses smart grid technology to aggregate DERs and manages them as a single power plant to participate in different electrical markets, such as the pool and futures markets, and supply electrical demand. The VPP can manage DERs from both commercial and technical aspects. The commercial virtual power plant (CVPP) gathers the economical parameters of its DERs and estimates market participants' strategies in order to maximize the VPP's profit in electricity markets. On the other hand, the technical virtual power plant (TVPP) ensures the safe operation of VPP by considering DERs' technical constraints (e.g. minimum and maximum generation, operation status) and network limitations (e.g. distribution lines power flow) [5].

The VPP operator must schedule its units in a specific period, such as daily or weekly [6]. In weekly scheduling, the VPP has the opportunity to participate in the futures market and signs forward contracts. Unlike the DA market, the futures market prices are certain, but they are usually lower than DA market prices. The various features of these markets help the VPP operator to increase its profit by participating in the DA market and reduce the risk of price fluctuations by participating in the futures market. Although medium-term scheduling provides an opportunity for VPP to participate in the futures market, it increases the probability of unit failure, which has a significant impact on VPP's profit. Therefore, it is essential to consider the impact of the failure of commonly used units to avoid the consequences [7].

1.2 | Literature review

The concept of VPP is utilized in many papers to aggregate DERs for the sake of many purposes. In [8], a VPP with high penetration of plug-in hybrid electric vehicles (PHEV) is developed to minimize operation cost. In [9], a VPP including wind power plant (WPP), photovoltaic (PV), combined heat and power (CHP), micro-turbine (MT), boiler, ESS, and buffer tank is presented that participates in the energy and spinning reserve markets to increase daily profits. A bi-level optimization model for the coordinated operation of electricity and gas networks is presented in [10]. This study utilized a VPP to manage electricity loads as demand response program. The authors of [11] developed a block chain based VPP in the distribution network that can manage its DERs in a decentralized manner. In [12], an optimal bidding strategy model is proposed for a VPP to participate in the DA, spinning reserve, and ancillary service markets. A VPP is modelled in [13], including RES, ESS, CHP, and a boiler in order to reduce environmental pollution by promoting the VPP management.

According to the reference [14], many articles in recent years are studied the participation of VPP in the pool market. In [15], a VPP is considered to represent a stochastic scheduling problem in which VPP can participate in the electric and thermal DA markets and supply electrical and thermal loads to maximize the profit. A scheduling problem for VPPs in a competitive environment with EV penetration is presented in [16]. The problem in [16] is bi-level in which VPPs goal is offering a proper strategy to attract more EVs in their parking lots to increase their revenues in the DA and reserve markets. A two-stage stochastic problem for a VPP, including DGs and FLs, is presented in [17]. The VPP in [17] attempts to present its optimal bidding/offering strategy for the DA, real-time, and spinning reserve markets. Although the VPP participation in the pool market is studied in the prior papers, in none of them the VPP participation in the futures market is investigated.

In recent years, in just some limited research works, the participation of VPP in the futures market is considered [14]. The futures market, also known as the Derivatives Exchange (DX), is a market in which electric power is traded at today prices and delivered in the future. This market has different contracts such as forward, swap, and option. It should be noted that the contract period of futures market varies from 1 week to several years. The main purpose of this market is to reduce financial risk due to high price volatility in the pool market [18–20]. In [21], a risk-averse two-stage stochastic model is presented for the participation of the VPP in the DA market, futures market, and contracts with withdrawal penalty (CWP). This paper aims to optimize the management of electrical and thermal units over a short-term time horizon to maximize the VPP's profit. In [18], a risk-constrained two-stage problem with a medium-term time horizon is presented in which the VPP can form an optimal coalition of DERs. The main purpose of the VPP in [18] is to maximize its profit by participating in pool and futures markets and signing bilateral contracts. A risk-constrained two-stage stochastic problem is modelled with a long-term time horizon in [19]. In this study, the VPP can compete with other VPPs by offering a reasonable rental rate for DERs. By using the rented DERs, VPP can participate in DA and futures markets and sign bilateral contracts to increase the profit. The VPP is modelled as single bus in [18, 19, 21]; therefore, the technical constraints of the distribution network (e.g. network topology and lines power flow limitations) are not taken into account. In addition, the time horizon in [18] and [19] is considered as medium- and long-term periods, respectively. Although medium- and long-term time horizons introduce the risk of VPP unit failure in the problem, the uncertainty caused by unit failure is not addressed in [18] and [19].

There are many uncertain parameters in VPP models due to the existence of multiple DERs and participation in different energy markets. The most important uncertainty parameters in VPP models include generated power of RES, failure of commonly used units, energy market prices, and electrical load. The widely used methods for handling the uncertainties are robust optimization [22], scenario generation and reduction [23], Monte Carlo simulation [24], point estimation method [25], and hybrid robust/stochastic method [26]. In order to use each of the mentioned uncertainty handling methods, some information related to the uncertainty parameters is required. This information can be the forecasted data, the statistical data, or the limit of these parameters. For example, the forecasted data of DA market prices are required to generate scenarios for this parameter. In this regard, the data should be obtained using time series prediction methods. In addition, a more precise forecasting method can lead to more accurate results. Thus, the number of scenarios and computational burden will be reduced. However, in the above-mentioned papers, the prediction of uncertainty parameters using time series prediction methods is ignored, and these papers have used theoretical information as forecasted data. Therefore, the forecast error of uncertainty parameters is unknown, and the highest forecast error should be considered to cover the uncertainty, which increases the problem's computational burden. It should be noted that forecast error varies for different uncertainty parameters, and each parameter uncertainty can be covered according to its forecast error. In other words, a parameter with a lower forecast error requires fewer scenarios to cover its uncertainty. Consequently,

TABLE 1 Comparison of the reviewed research works.

	Market			Formulation type		Uncertainty parameters						
Ref.	Pool	Futures	Network	Determ-inistic	Stochastic	Load	Price	Wind speed	Radiation	Unit failure	Uncertainty method	Risk man-agement
[9]	✓				✓	✓	✓	✓	✓		SG	Downside risk
[10]	✓		✓	✓							—	—
[12]	✓		✓	✓							—	—
[15]	✓		✓		✓	✓	✓	✓	✓		SG	—
[17]	✓		✓		✓	✓	✓	✓			SG	CVaR
[21]	✓	✓			✓	✓	✓	✓			SG	CVaR
[18]	✓	✓			✓		✓	✓	✓		SG	CVaR
[19]	✓	✓			✓	✓	✓				SG	CVaR
[22]	✓				✓			✓	✓		Robust	—
[24]	✓		✓		✓	✓		✓			Monte Carlo	—
[26]	✓				✓	✓	✓	✓			Hybrid robust/stochastic	—
This paper	✓	✓	✓		✓	✓	✓	✓	✓	✓	LSTM + SG	CVaR

Abbreviations: CVaR, conditional value at risk; LSTM, long short-term memory; SG, scenario generation.

it is a more reasonable methodology to predict the uncertainty parameters first and then capture the uncertainty based on the forecast error. This can ensure that the results of the problem are more accurate and reduce the computational burden.

The reviewed papers in this section are summarized in Table 1. This table is designed based on market participation, network modelling, formulation type, risk measurement, and uncertainty handling methods.

1.3 | Research gaps and contributions

The participation of the VPP in the futures market not only reduces the risk caused by the price fluctuations of the DA market but also provides an arbitrage opportunity for the VPP's operator. Despite these advantages, few recent studies have investigated the participation of the VPP in the futures market. Although the VPP's involvement in the futures market is considered in [18] and [19], the constraints of the distribution network, such as the power flow and the location of the units, are not taken into account. In other words, in these studies, the VPP is modelled from a commercial point of view, and its technical constraints are not examined. The participation of the VPP in the futures market requires medium/long-term scheduling, which creates uncertainty related to the failure of commonly used units. If this uncertainty is not considered, a portion of the loads will be lost, and the costs of the VPP will increase. The uncertainty related to the failure of commonly used units is not considered in any of the papers mentioned above.

To fill the mentioned research gaps, here, the optimal bidding strategy of VPP for participating in the pool and futures markets is modelled as a two-stage risk constrained stochastic problem. Moreover, the commercial and technical aspects of the VPP such as distribution network constraints and the impact of unit failure are investigated. It should be mentioned that by participating in the futures market, the VPP reduces its financial risk and provides an arbitrage opportunity. In what follows, the contributions of this paper are expressed:

- Modelling a two-stage optimal bidding strategy for a technical and commercial VPP to participate in futures and pool markets considering risk constraints through the conditional value at risk (CVaR) method.
- Investigating the impact of unit failure on VPP's profit and risk of the problem in the proposed model.
- Utilizing a hybrid method of LSTM neural network and scenario generation and reduction to handle problem uncertainty in the presence of actual uncertainty data.
- Arbitrage modelling as a VPP trading strategy on different energy trading floors available in the energy markets.

The rest of this paper is organized as follows. Section 2 describes the model framework, including the VPP and market structure. Section 3 discusses uncertainty modelling. Sections 4 and 5 present the problem formulation and the numerical results, respectively. Finally, the paper is concluded in Section 6.

2 | MODEL FRAMEWORK

A VPP including DG, ESS, WPP, PV, and FL units is proposed here. As shown in Figure 1, the proposed VPP has two units for each technology, which are distributed throughout a radial network. It is also assumed that the VPP operator owns all network units and controls them centrally. According to Figure 1, the VPP is connected to the upstream network through node

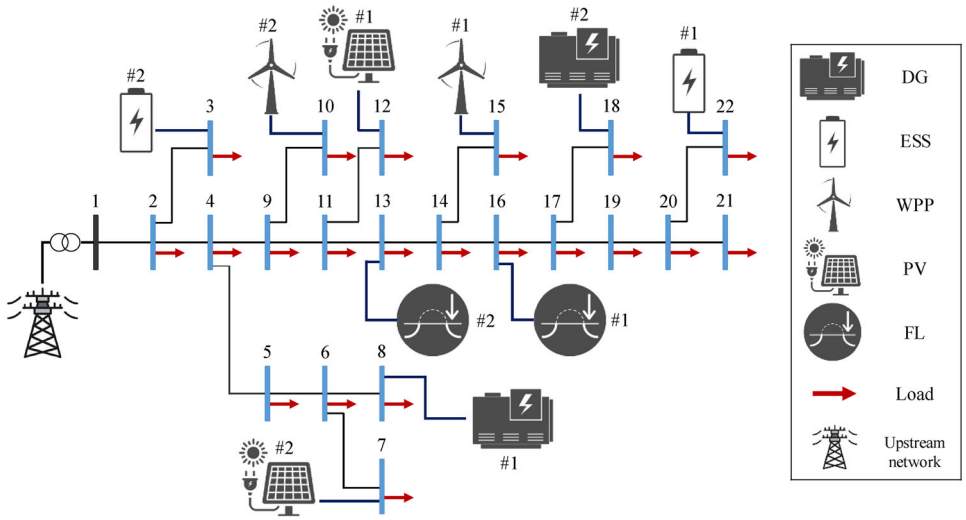

FIGURE 1 The overall structure of the proposed virtual power plant. DG, distributed generation; ESS, energy storage systems; FL, flexible loads; PV, photovoltaic; WPP, wind power plant.

1 and can trade power with the pool and futures markets. In this study, the VPP can signs the forward contracts of futures market. For the sake of simplicity and to prevent the extra computational complexity of the problem, the DA market is chosen among the pool markets.

The proposed model is formulated as a two-stage stochastic problem. In the first stage, the VPP signs forward contracts in the futures market, and in the second stage, the VPP manages its units and participates in the DA market. It should be noted that the network loads are also supplied at this stage. The first stage variables are scenario-independent, while the second stage variables are scenario-dependent. Moreover, the time horizon of the problem is one week with hourly intervals. It is noteworthy that the VPP will participate in the DA market as a price taker. As mentioned earlier, the time horizon of the problem in this study is 1 week. Therefore, DA market prices are predicted for all hours of the under study week, and different scenarios are generated to cover the uncertainty of the prices by the VPP operator.

3 | UNCERTAINTY CAPTURING

3.1 | Uncertainty capturing of time series

Here, to capture the uncertainty of electrical load, DA market prices, wind speed, and solar radiation, data prediction using LSTM neural network and scenario generation is utilized. LSTM neural network is a recurrent neural network that can learn short- and long-term temporal dependencies between data without getting stuck in a gradient vanishing problem. Figure 2 shows an LSTM unit's structure consisting of a cell state and three gates, including forget, input, and output. The LSTM unit can add and remove information from the cell state using its gates. In fact, gates control the information stored in the cell state. The forget gate removes unnecessary information from the cell state. The input gate stores crucial new information in the cell state. This gate identifies important new information and then adds a coefficient of this information to the cell state. The new cell state (c_t) is updated using the forget and input gates. Finally, the output gate specifies the output information of the LSTM unit. The hidden state (h_t) is the filtered version of the cell state [12, 27, 28]. The formulation of the LSTM network is presented in Equations (1)–(6):

$$f_t = \sigma\left(W^f x_t + U^f h_{t-1} + b^f\right), \tag{1}$$

$$i_t = \sigma\left(W^i x_t + U^i h_{t-1} + b^i\right), \tag{2}$$

$$o_t = \sigma\left(W^o x_t + U^o h_{t-1} + b^o\right), \tag{3}$$

$$\tilde{c}_t = \tanh\left(W^c x_t + U^c h_{t-1} + b^c\right), \tag{4}$$

$$c_t = f_t \odot c_{t-1} + i_t \odot \tilde{c}_t, \tag{5}$$

$$h_t = o_t \odot \tanh\left(c_t\right). \tag{6}$$

The variables W, U and b that are determined during the neural network training process are the input weight matrix, the recurrent connection weight matrix, and the bias vector, respectively. c_t is the cell state variable and the variables f_t, i_t and o_t are forget, input, and output gates, respectively. x_t is the input vector of the LSTM unit, and h_t is the related output vector. It should be noted that the symbols σ, tanh and $\odot$ are the sigmoid activation function, the hyperbolic tangent activation function, and the element-wise multiplication function, respectively.

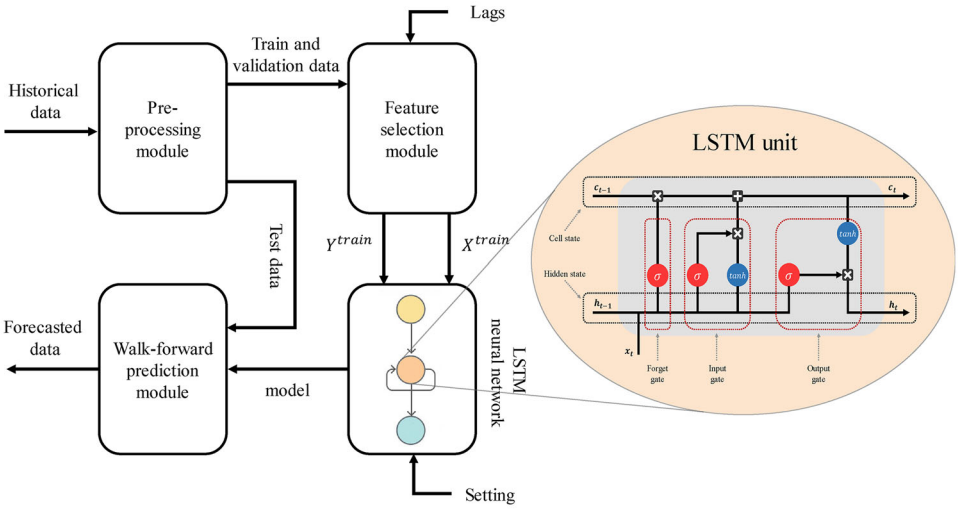

FIGURE 2 The overall structure of data prediction using LSTM neural network. LSTM, long short-term memory.

Figure 2 shows the overall structure of data prediction. First, historical data is imported into the pre-processing module. In this module, filling in missing data, splitting the data into training, validation and test sets, and normalizing the data are done. Second, the training and validation data is imported into the feature selection module. In this step, applying lag on the training and validation data makes this data suitable for supervised learning. Then, we apply input (X^{train}) and output data (Y^{train}) along with the settings to the LSTM neural network. The main settings of the LSTM neural network include the number of hidden layers, the number of neurons in each layer, the learning rate, and the optimization algorithm. In this step, the neural network learns the pattern between training data and builds a model for it. Finally, test data and the model are applied to the prediction module to obtain the forecasted data using the walk-forward method [29]. After the forecasted data are obtained, several scenarios are generated using their probability density functions (PDFs) [30]. It should be noted that there are a considerable number of uncertainty parameters in this problem; consequently, it is possible to skip generating scenarios for parameters with an acceptable forecast error to decrease the computational burden of the problem. In other words, the indicated prediction method ensures that the uncertainty associated with these parameters is covered. For other parameters with a high forecast error, numerous scenarios are generated. Then, these scenarios are reduced using the Kmeans method to decrease the computational burden of the problem [31].

3.2 | Uncertainty capturing of DG units

Scenario generation to demonstrate the availability state of the generation unit requires two parameters, mean time to repair (MTTR) and mean time to failure (MTTF). These two parameters are determined based on the technology of each generation unit. The time between two consecutive failures and the time required to repair the unit's failure follow an exponential distribution which is defined as the following equations.

$$t_F = -\text{MTTF} \times \ln(u_1) \tag{7}$$

$$t_R = -\text{MTTR} \times \ln(u_2) \tag{8}$$

In (7) and (8), u_1 and u_2 are random numbers between 0 and 1 that is generated using a uniform distribution. As a result, different values for t_F and t_R are employed to show the state of the generation unit. Figure 3 represents a generated scenario for a DG unit. According to this figure, $t_F^{(i)}$ represents the time for the i^{th} failure to occur, and $t_R^{(i)}$ represents the time to repair the i^{th} failure. Further information about the modelling of this method is available in [7, 32].

4 | PROBLEM FORMULATION

The optimal bidding strategy of VPP is modelled as a two-stage stochastic problem with a 1-week time horizon. In the first stage, the VPP operator adjusts its contracts with the futures market for the following week. In the second stage, the optimal exchanged power of the VPP with the DA market and the optimal generation of the VPP units are determined. Various uncertainty parameters can be considered in the proposed model, including the high price volatility of the DA market and the impact of unit failure, as the riskiest ones. These uncertainties can increase the standard deviation of VPP profit, which is required to be reduced using the risk management technique. The CVaR risk measure is used to make a trade-off between the expected profit of VPP and the risk [33]. The problem

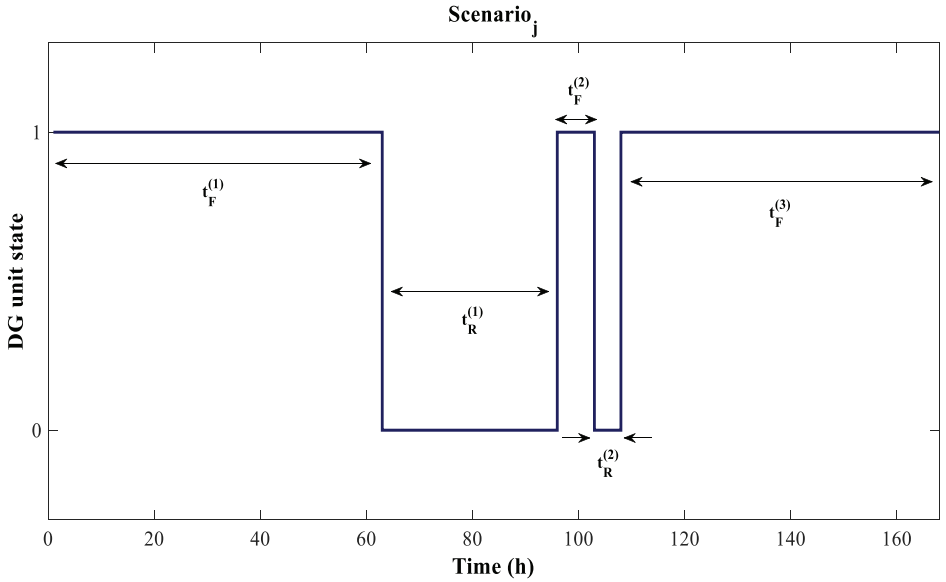

FIGURE 3 Availability scenario of a DG unit. DG, distributed generation.

formulations are expressed as follows.

$$\max OF = (1-\beta) \times \left[R^{DX} + \sum_s \pi_s \times \left(R_s^{DA} + R_s^{Retail} - C_s^{DER} \right) \right] + \beta \times \left[\xi - \frac{1}{1-\alpha} \times \sum_s \pi_s \times \eta_s \right] \quad (9)$$

$$R^{DX} = \sum_c \sum_b \sum_t \left(P_{c,b,t}^{DX,sell} \times \lambda_{c,b}^{DX,sell} - P_{c,b,t}^{DX,buy} \times \lambda_{c,b}^{DX,buy} \right) \times \Delta t \quad (10)$$

$$R_s^{DA} = \sum_t P_{t,s}^{DA} \times \lambda_{t,s}^{DA} \times \Delta t \qquad \forall s \in \Omega_S \quad (11)$$

$$R_s^{Retail} = \sum_i \sum_t PD_{i,t,s} \times \lambda^{Retail} \qquad \forall s \in \Omega_S \quad (12)$$

$$C_s^{DER} = C_s^{DG} + C_s^{ESS} \qquad \forall s \in \Omega_S \quad (13)$$

The objective function is given in (9) consists of two parts. In the first part, the expected profit of VPP is maximized, and in the second part, the CVaR is included to represent the risk aversion of the VPP operator. The expected profit of VPP includes the profit obtained from the futures market, the profit obtained from the DA market, the expected retail revenue and operation cost of units, respectively. As β increases to 1, the problem becomes more conservative and less risky. Furthermore, if β becomes zero, it will be risk-neutral. The chosen value of β depends on the decision of the VPP operator.

The VPP revenue from the futures market is equal to the total profit from the sale of power minus the total cost of purchasing power in the contracts of this market, presented in (10). In (11) and (12), VPP revenue from the DA market and VPP retail revenue are defined, respectively. If FLs reduce their load demand, retail revenue is reduced. Consequently, the VPP tries to supply all of its load and avoids load curtailment as much as possible. In (13) the operation cost of DG and ESS units in each scenario is presented.

$$P_{c,b,t}^{DX} = P_{c,b,t}^{DX,sell} - P_{c,b,t}^{DX,buy} \; \forall c \in \Omega_C, b \in \Omega_B, t \in \Omega_T, \quad (14)$$

$$P_{c,b,t}^{DX,sell} = u_{c,b,t}^{DX,sell} \times P_{c,b}^{DX,Block} \; \forall c \in \Omega_C, b \in \Omega_B, t \in \Omega_T, \quad (15)$$

$$P_{c,b,t}^{DX,buy} = u_{c,b,t}^{DX,buy} \times P_{c,b}^{DX,Block} \; \forall c \in \Omega_C, b \in \Omega_B, t \in \Omega_T, \quad (16)$$

$$u_{c,b,t}^{DX,sell} \le TC_{c,t}^{DX} \; \forall c \in \Omega_C, b \in \Omega_B, t \in \Omega_T, \quad (17)$$

$$u_{c,b,t}^{DX,buy} \le TC_{c,t}^{DX} \; \forall c \in \Omega_C, b \in \Omega_B, t \in \Omega_T, \quad (18)$$

$$u_{c,b,t}^{DX,sell} + u_{c,b,t}^{DX,buy} \le 1 \; \forall c \in \Omega_C, b \in \Omega_B, t \in \Omega_T, \quad (19)$$

$$u_{c,b,t}^{DX,sell} \ge u_{c,b+1,t}^{DX,sell} \; \forall c \in \Omega_C, b \in \Omega_B, t \in \Omega_T, \quad (20)$$

$$u_{c,b,t}^{DX,buy} \ge u_{c,b+1,t}^{DX,buy} \; \forall c \in \Omega_C, b \in \Omega_B, t \in \Omega_T. \quad (21)$$

In (14)–(21), the related constraints of futures market are defined. The quantity of power traded with the futures market is formulated in Equation (14). The first term on the right-hand-side of (12) represents the sale of power, and the second term represents the purchase of power from this market. In (15) and (16), the number of sold and purchased power blocks in each contract is specified. According to (17) and (18), trading in futures markets contracts is permitted only during certain hours. For instance, the peak contract is only signed during peak hours. In (19), simultaneous signing of the sales and purchase contract is avoided. The constraints in (20) and (21) indicate the priority of block b over block b+1. These constraints indicate that the blocks of each contract in the futures market must be traded

in order. It should be noted that according to the equality that exists in (15) and (16), the existence of (20) and (21) is necessary for the futures market blocks to be traded in order. If (20) and (21) did not exist, the VPP could, for example, buy the second block of futures market contracts without buying the first block of that contract.

$$P^{DA}_{t,s} = P^{DA,sell}_{t,s} - P^{DA,buy}_{t,s} \; \forall t \in \Omega_T, s \in \Omega_S, \tag{22}$$

$$P^{DA,sell}_{t,s} \le P^{DA,max} \times u^{DA,sell}_{t,s} \; \forall t \in \Omega_T, s \in \Omega_S, \tag{23}$$

$$P^{DA,buy}_{t,s} \le P^{DA,max} \times u^{DA,buy}_{t,s} \; \forall t \in \Omega_T, s \in \Omega_S, \tag{24}$$

$$u^{DA,sell}_{t,s} + u^{DA,buy}_{t,s} \le 1 \; \forall t \in \Omega_T, s \in \Omega_S. \tag{25}$$

In (22)–(25) the power exchange between the VPP and the DA market is modelled. Equation (22) represents the amount of power exchanged in this market. The constraints in (23) and (24) indicate the amount of sold and purchased power. The constraint in (25) stands for preventing simultaneous trading in the DA market. It should be noted that the purchase and sale amounts of the DA market are defined separately to prevent the VPP from using the arbitrage opportunity.

$$u^{DA,buy}_{t,s} + u^{DX,sell}_{c,b,t} \le 1 \; \forall t \in \Omega_T, s \in \Omega_S, c \in \Omega_C, b \in \Omega_B, \tag{26}$$

$$u^{DA,sell}_{t,s} + u^{DX,buy}_{c,b,t} \le 1 \; \forall t \in \Omega_T, s \in \Omega_S, c \in \Omega_C, b \in \Omega_B, \tag{27}$$

$$u^{DX,buy}_{c,b,t} + u^{DX,sell}_{c',b',t} \le 1 \; \forall c \in \Omega_C, b \in \Omega_B, b' \in \Omega_B, t \in \Omega_T, c' \in \Omega_C. \tag{28}$$

The constraints in (26)–(28) are defined to prevent the VPP from taking advantage of the arbitrage opportunity. According to (26) and (27), the VPP cannot purchase electricity from the DA/futures market and then sell it to the futures/DA market. Moreover, the constraint in (28) indicates that the VPP is unable to buy from one of the power blocks of contract c and then sell to another power block of contract c'. It should be noted that c' is defined so that the VPP cannot benefit from the price difference between futures market contracts. Consequently, the VPP is unable to take advantage of price differences between the electricity markets. It should be emphasized that (28) differs from (19). The purpose of (28) is that the VPP cannot benefit from the price difference between different contracts. In contrast, the purpose of (19) is that the VPP cannot simultaneously buy and sell a specific block of a specific contract.

$$\sum_{wpp \in \Omega_{WPP}} P^{i}_{wpp,t,s} + \sum_{pv \in \Omega_{PV}} P^{i}_{pv,t,s} + \sum_{ess \in \Omega_{ESS}} P^{i}_{ess,t,s} + \sum_{dg \in \Omega_{DG}} P^{i}_{dg,t,s} = PD_{i,t,s} + \sum_{c} \sum_{b} P^{DX}_{c,b,t} + P^{DA}_{t,s} + \sum_{j \in \Omega_I} flow_{i,j,t,s} \quad \forall i \in \Omega_I, t \in \Omega_T, s \in \Omega_S, \tag{29}$$

$$\underline{flow}_{i,j,t,s} S^{base} = B^{line}_{i,j} \times \left(\delta_{i,t,s} - \delta_{j,t,s}\right) \; \forall i, j \in \Omega_I, t \in \Omega_T, s \in \Omega_S, \tag{30}$$

$$PD_{i,t,s} = Load_{i,t,s} - \sum_{fl} P^{i}_{fl,t,s} \; \forall i \in \Omega_I, t \in \Omega_T, s \in \Omega_S. \tag{31}$$

The power balance constraint is defined in Equation (29). The power flow of lines and the demand of each node are represented in (30) and (31), respectively.

$$C^{DG}_{s} = \sum_{dg} \sum_{k} \sum_{t} a_{dg,k} \times Pg_{dg,t,s,k} \; \forall s \in \Omega_S, \tag{32}$$

$$Pg_{dg,t,s,k} \le P^{max}_{dg,k} \; \forall dg \in \Omega_{DG}, k \in \Omega_K, t \in \Omega_T, s \in \Omega_S, \tag{33}$$

$$P_{dg,t,s} = \sum_{k} Pg_{dg,t,s,k} \; \forall dg \in \Omega_{DG}, t \in \Omega_T, s \in \Omega_S, \tag{34}$$

$$P^{min}_{dg} \times u_{dg,t,s} \times UA_{dg,t,s} \le P_{dg,t,s} \le P^{max}_{dg} \times u_{dg,t,s} \times UA_{dg,t,s} \; \forall dg \in \Omega_{DG}, t \in \Omega_T, s \in \Omega_S, \tag{35}$$

$$P_{dg,t,s} - P_{dg,t-1,s} \le RU_{dg} \; \forall dg \in \Omega_{DG}, t \in \Omega_T, s \in \Omega_S, \tag{36}$$

$$P_{dg,t-1,s} - P_{dg,t,s} \le RD_{dg} \; \forall dg \in \Omega_{DG}, t \in \Omega_T, s \in \Omega_S. \tag{37}$$

The constraints in (32)–(37) are related to the technical and economic constraints of DG units. In (32), the total operation cost of DG units is calculated. The capacity of each DG unit is divided by k power blocks, and the price of each power block is increased ascendingly. Consequently, DG operation costs can be modelled linearly. In (33), the power of each block is bounded, and the total generation of each DG unit is considered in (34). The constraint in (35) represents DG units' minimum and maximum generation limits. In this constraint, the failure status of each unit is determined by the parameter $UA_{dg,t,s}$. When $UA_{dg,t,s}$ equals zero, the unit fails, and when it equals one, the unit is working. In other words, this equation determines each DG unit's on or off status and failure status. In order to model the ramp rates of DG units, the constraints in (36) and (37) are represented.

$$C^{ESS}_{s} = \sum_{ess} \sum_{t} a_{ess} \times \left(P^{dch}_{ess,t,s} + P^{ch}_{ess,t,s}\right) \quad \forall s \in \Omega_S, \tag{38}$$

$$P_{ess,t,s} = P^{dch}_{ess,t,s} - P^{ch}_{ess,t,s} \quad \forall ess \in \Omega_{ESS}, t \in \Omega_T, s \in \Omega_S, \tag{39}$$

$$P^{dch}_{ess,t,s} \le P^{dch,max}_{ess} \times u^{dch}_{ess,t,s} \quad \forall ess \in \Omega_{ESS}, t \in \Omega_T, s \in \Omega_S, \tag{40}$$

$$P^{ch}_{ess,t,s} \le P^{ch,max}_{ess} \times u^{ch}_{ess,t,s} \quad \forall ess \in \Omega_{ESS}, t \in \Omega_T, s \in \Omega_S, \tag{41}$$

$$u^{dch}_{ess,t,s} + u^{ch}_{ess,t,s} \le 1 \quad \forall ess \in \Omega_{ESS}, t \in \Omega_T, s \in \Omega_S, \tag{42}$$

$$SOC_{ess,t,s} = SOC_{ess,t-1,s} + \left(P^{ch}_{ess,t,s} \times \eta^{ch}_{ess} - P^{dch}_{ess,t,s} / \eta^{dch}_{ess}\right) \times \Delta t \quad \forall ess \in \Omega_{ESS}, t \in \Omega_T, s \in \Omega_S, \tag{43}$$

$$(1 - DOD_{ess}) \times SOC_{ess}^{max} \times \Delta t \leq SOC_{ess,t,s} \leq SOC_{ess}^{max} \times \Delta t \quad \forall ess \in \Omega_{ESS}, t \in \Omega_T, s \in \Omega_S. \tag{44}$$

The constraints related to ESS modelling are given in (38)–(44). The constraint in (38) calculates the degradation cost of the ESS. In (39), the total power of ESS is defined. The discharging and charging power of ESS are bounded in (40) and (41), respectively. The constraint in (42) prevents simultaneous charging and discharging of ESS. The state of charge (SOC) of each ESS is formulated in (43) and bounded in (44).

$$P_{fl,t,s} \leq P_{fl}^{max} \quad \forall fl \in \Omega_{FL}, s \in \Omega_S \tag{45}$$

The maximum power that each FL can curtail is defined in (45).

$$\xi - \left(R^{DX} + R_s^{DA} + R_s^{Retail} - C_s^{DER}\right) \leq \eta_s \quad \forall s \in \Omega_S \tag{46}$$

$$\eta_s \geq 0 \quad \forall s \in \Omega_S \tag{47}$$

The risk modelling is represented in (46) and (47). The variable ξ represents value at Risk (VaR), and η is a non-negative variable equal to the difference between VaR and VPP profit. If the profit of VPP is smaller than ξin scenario s, the value of ηbecomes positive; otherwise, it is zero.

The proposed VPP bidding strategy modelling problem is illustrated in Figure 4. As can be seen in this figure, the presented model includes three parts. In the first part, the historical data of uncertainty parameters are given to the LSTM neural network to be predicted. The forecasted parameters and DG unit information are given to the scenario generation and reduction module in the second part. In the last part, the generated scenarios are applied to the optimization problem to solve the MILP problem.

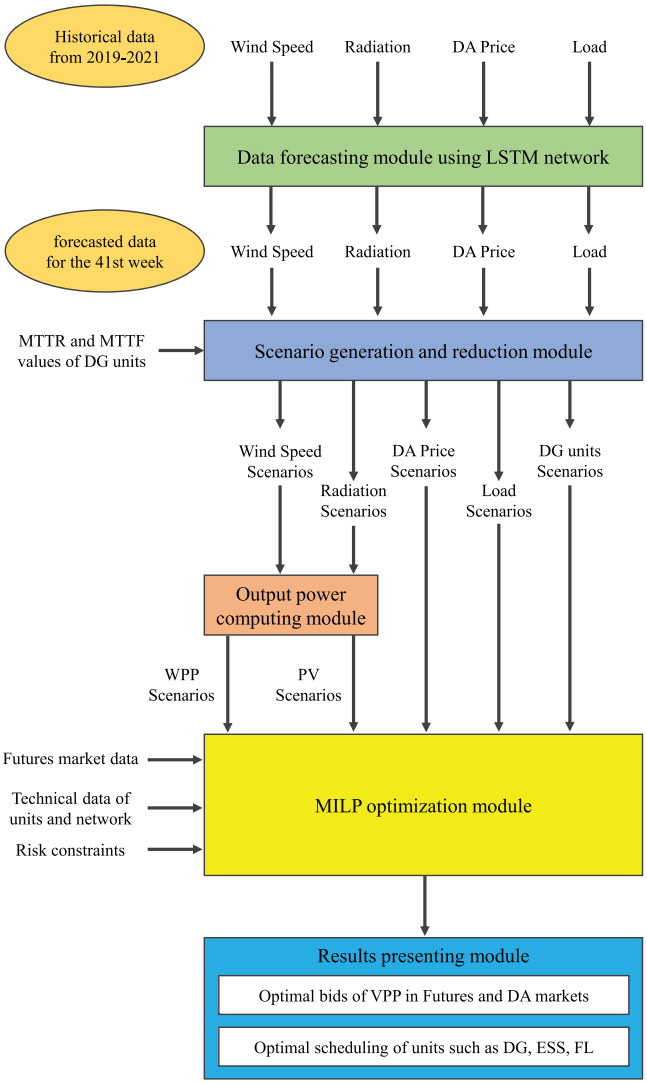

FIGURE 4 Schematic modelling of the proposed virtual power plant (VPP) optimal bidding strategy problem. DA, day-ahead; DG, distributed generation; ESS, energy storage systems; FL, flexible loads; MTTR, mean time to repair; MTTF; mean time to failure; WPP, wind power plant.

5 | NUMERICAL RESULTS

5.1 | Input data

The required input data can be divided into two parts, data related to neural network training and data related to the optimization problem. The training data for neural networks includes historical data of uncertainty parameters and neural network settings. Here, the considered uncertainty parameters are electrical loads, DA market price, wind speed and solar radiation. The input data for the considered uncertainty parameters is derived from Spain electricity demand [34], Spain DA market prices (OMIP) [35], and the Brownfield meteorological station in Texas [36], respectively. Since the data used in this research are real data, they are correlated with each other; therefore, the generated scenarios are affected by this correlation. For instance, changes in the DA market prices and electrical loads usually happen simultaneously. This is also true for wind speed and solar radiation data. Additionally, to fit the model, the electricity load data is scaled down to 1:1500. The input data is collected on an hourly resolution from 1 January 2019 to 31 December 2021. The LSTM network is configured so that the previous 48-h data are used as inputs for predicting each data. Additionally, the data are divided into three parts; Train, Validation, and Test, which represent 80%, 10% and 10% of the total data, respectively. The LSTM network is trained using train and validation data, and test data is used to assess its performance. Moreover, the mini-batch technique and L2-regularization are utilized to accelerate the training process and avoid over-fitting. In order to evaluate the performance of the LSTM network, error indices such as mean absolute error (MAE), root mean squared error (RMSE), and mean absolute percentage error (MAPE) are considered. Finally, the 41st week of 2021 (11 October to 17 October) is

selected from the forecasted data as the sample week for the optimization problem.

There are different technologies within the VPP, such as DG, ESS, WPP, PV and FL, and each of these technologies consists of two units. The capacities of first and second DG unit are equal to 6 and 5 MW, respectively. WPP units are considered to be 6 and 9 MW. PV units have a capacity of 4 and 6 MW, and FLs are assumed to handle 0.5 and 1 MW. Further technical and economic data of DGs, FLs and ESS are extracted from [19] and [20]. Similarly, WPPs and PV technical data are derived from [15] and [33], respectively. In order to evaluate the effectiveness of proposed model, a 22-node radial network is considered as the test system [38].

The VPP can sign base and peak contracts in the futures market. The rules used to implement the futures market in this study are similar to those presented in [6], [29], and [35]. Base and peak contracts can be signed at off-peak and peak hours of the week, respectively. Note that 8–11 am and 7–11 pm are considered to be daily peak hours. According to [18], each contract consists of four purchase and sale power blocks, and the amount of the power blocks is equal to 2.5, 5, 7.5, and 10 MW. The selling and buying prices are the same in the first power block, and these prices have been selected based on the Spain futures market for the 41st week of 2021 [40]. The price of other purchase/sale power blocks increases/decreases gradually with a certain percentage [18]. It should be noted that the peak contract price is always higher than the base contract price.

The DA market price was derived from the Spanish spot market price from 11 October to 17 October 2021 [35]. As mentioned, this paper assumes that the DA market price is constant and is not updated during the days of the week. According to [41], the retail price is assumed as 281 $\frac{€}{MWh}$.

In order to model the failure of DG units, data on MTTF and MTTR is required. According to the technology of these units, the MTTF and MTTR are selected as 450 and 50 h, respectively [42]. It should be noted that in risk modelling, the value of the confidence level (α) is equal to 0.9.

The LSTM network is implemented using Python 3.9 software and the Keras and Tensorflow libraries [43–45]. The optimization algorithm used for training the network is Adam, which is one of the most widely used solvers in deep learning applications [46]. The mixed-integer linear programming (MILP) formulation of the proposed model is optimized in GAMS 24.3 software using the CPLEX 12.6 solver [43] and [44], over a personal system with a 3.0 GHz corei7 CPU and 64GB of RAM.

5.2 | Simulation results

In this section, the obtained results of proposed optimal bidding strategy of the VPP in a weekly time horizon are presented. The problem is formulated as both deterministic and stochastic models. In the deterministic case, the LSTM network performance is evaluated. Several scenarios and risk constraints model the problem in stochastic cases. Additionally, the impacts of unit failure and arbitrage opportunity are considered in stochastic cases. The following cases are considered to investigate the effectiveness of proposed model.

TABLE 2 Evaluation of LSTM neural network performance using MAE, RMSE, and MAPE indices.

Error criteria	Load (MW)	Price (Euro/MWh)	Wind speed (m/s)	Radiation (kW/m^2)
MAE	518.501	10.379	0.662	0.037
RMSE	655.027	15.14	0.905	0.056
MAPE (%)	1.94	9.631	7.106	—

Abbreviations: LSTM, long short-term memory; MAE, mean absolute error; RMSE, root mean squared error; MAPE, mean absolute percentage error.

- Case 1: Deterministic problem of optimal bidding strategy of VPP
- Case 2: Two-stage stochastic problem of optimal bidding strategy of VPP considering risk constraints
- Case 3: Case 2 and considering the impact of DG units' failure
- Case 4: Case 3 and considering arbitrage opportunity

5.2.1 | Case 1

In this case, a deterministic problem is modelled using (9)–(45) without considering scenarios and risk constraints. Then, the problem is solved by comparing two sets of forecasted and actual data of uncertainty parameters to determine the difference between the obtained results. Figure 5 shows the prediction results of the uncertainty parameters using the LSTM network as well as their actual values. It should be noted that the scenarios depicted in Figure 5 are not taken into account in this case. Based on the illustrated results, the LSTM network is able to predict the trend of each uncertainty parameter properly. Wind speed and solar radiation data are transformed into power and used to solve the optimization problem.

Table 2 displays various error indicators to evaluate the neural network performance. MAE, RMSE and MAPE are considered to measure the error between the forecasted and actual data. These indicators are discussed in [49]. As shown in Table 2, the MAPE is not calculated for solar radiation data due to the existence of zero values in this data.

The results of the deterministic problem using the forecasted and actual data are reported in Table 3. This table shows that the problem can be solved with and without considering constraints (26)–(28). By ignoring the constraints (26)–(28), the VPP can benefit from the price difference between DA and futures markets. The results of Table 3 indicate that the VPP profit error is low, and the LSTM network can predict the parameters accurately. It can be seen that VPP has a higher error when the arbitrage opportunity is considered. It is due to the high amount of exchanged power between VPP and the DA market that can lead to more error in the final forecasted data.

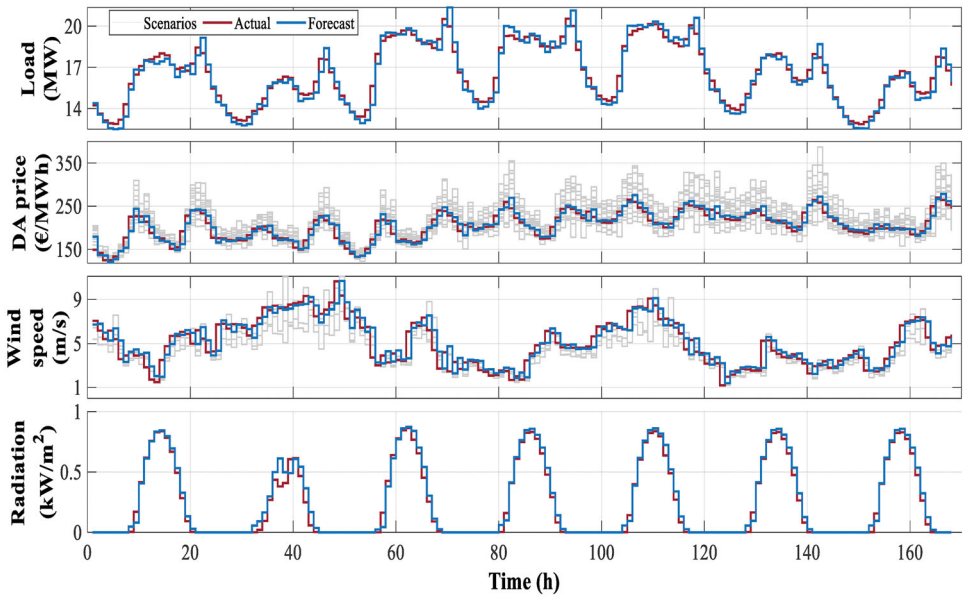

FIGURE 5 Actual and forecasted values of electricity loads, DA market price, wind speed, and solar radiation. DA, day-ahead.

The high accuracy of the LSTM network in predicting time series allows the VPP operator to propose a more precise strategy in the markets. Furthermore, accurate prediction of RES generation facilitates the high penetration of these units. One of the main purposes of this study is investigating the accuracy of LSTM network in uncertainties capturing and considering their impact on the optimization problem.

5.2.2 | Case 2

In this case, the problem is developed as a stochastic model and solved considering several scenarios. Due to considering many uncertainty parameters, scenario generation for all of these parameters will increase the computational burden of the optimization problem. In this regard, due to the low forecast error for electricity load and solar radiation (see Table 2), no scenario is generated for these parameters. On the other hand, based on Table 2, since the forecast error of wind speed and DA market prices is relatively high, 3 and 15 scenarios are generated for the wind speed and DA market prices, respectively. Thus, in this case the total number of scenarios is equal to $3 \times 15 = 45$.

TABLE 3 Numerical results of case 1 with and without considering arbitrage constraints for actual and forecasted data.

	With (24)–(26) constraints (no arbitrage)		Without (24)–(26) constraints (arbitrage)	
Parameters	**Actual**	**Forecasted**	**Actual**	**Forecasted**
Futures market revenue ($\times 10^3$ €)	56.170	58.478	305.765	274.418
DA market revenue ($\times 10^3$ €)	5.113	10.556	−193.411	−150.481
Retail revenue ($\times 10^3$ €)	780.124	775.731	781.958	777.591
DER cost ($\times 10^3$ €)	48.422	48.379	48.379	48.379
VPP net profit ($\times 10^3$ €)	792.985	796.339	845.8982	853.104
Error (%)	—	0.42	—	0.85

Abbreviations: DA, day-ahead; DER, distributed energy resource; VPP, virtual power plant.

The expected profit of the VPP, in this case, is equal to 810.203×10^3 €, which is calculated without considering the risk of fluctuation in the DA market prices. Figure 6 demonstrates the generation of VPP and its interaction with the DA and futures markets with $\beta = 0$. In this figure, positive and negative values indicate the sale and purchase of power, respectively. Furthermore, positive and negative values for the ESS are discharging and charging power, respectively. The generation of VPP shows that it acts as a dispatchable unit. For instance, at hour 41, the VPP generation exceeds its load, so VPP sells its surplus power to the upstream network. On the other hand, at hour 69 the amount of load consumed by VPP is greater than its generation, so the required extra power is delivered from the upstream network. At 4 o'clock, the load consumption and the DA market price are both low. Therefore, power is purchased from the DA market by VPP and used for charging ESS. In contrast, at hour 106, the load consumption and the DA market price are both high. In this regard, VPP reduces the FLs and discharges ESS to sell power to the DA market.

According to Figure 6, VPP often appears as a power seller in the base contract and as a power buyer in the peak contract. In general, VPP tries to sell its extra power to a market with a higher price and supply its required power by buying power from a market with a cheaper price. The required power

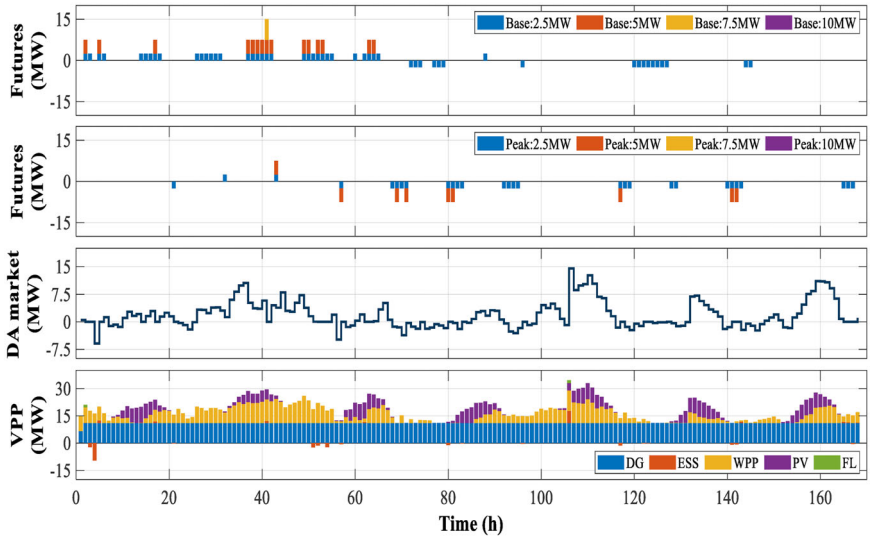

FIGURE 6 Generation of VPP and its interaction with DA and futures markets in case 2 with $\beta = 0$. DA, day-ahead; VPP, virtual power plant.

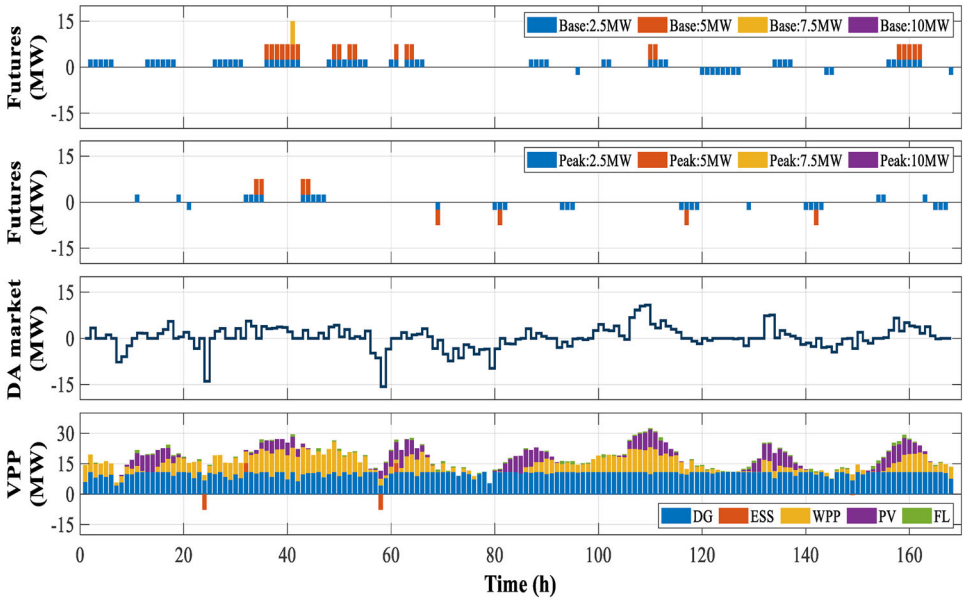

FIGURE 7 Generation of VPP and its interaction with DA and futures markets in case 2 and for $\beta = 1$. DA, day-ahead; VPP, virtual power plant.

of VPP can be supplied by both the DA and futures markets during certain week hours. For example, at hour 70, 2.5 and 3.64 MW of VPP required power are supplied by buying power from the futures and DA markets, respectively. This is because the power blocks of each futures market contract are constant. On the other hand, it is more economical for a VPP to supply the remaining power by buying power from the DA market than buying the next power block of the futures market. A similar situation occurs for selling power to markets (e.g. hour 43).

As mentioned, high fluctuations in DA market prices increase the risk of this problem. Therefore, the risk-averse problem will be solved if β is 1. In case 2, with $\beta = 1$, the expected profit of VPP and the amount of CVaR are equal to 771.503×10^3 € and 771.128×10^3 €, respectively. The power generation of VPP and its interaction with the DA and futures markets with $\beta = 1$ are illustrated in Figure 7. As shown, the amount of sold power in the base and peak contracts is increased. However, the amount of purchased power from futures market is decreased. For example, during hours 156 to 162, the amount of sold power in the base contract is increased, while at hours 57 and 71, the amount of purchased power from the peak contract is decreased. In general, the VPP interaction with the futures market is increased while it is decreased with the DA market. For instance, at hours 32 to 49, the amount of sold power to the DA market is decreased. The results of risk-averse problem show that by increasing β, due to the high price volatility, VPP tendency to participate in the DA market is reduced. Therefore, VPP prefers to exchange power with the futures market, which due to its constant prices is less risky. It should be noted that by

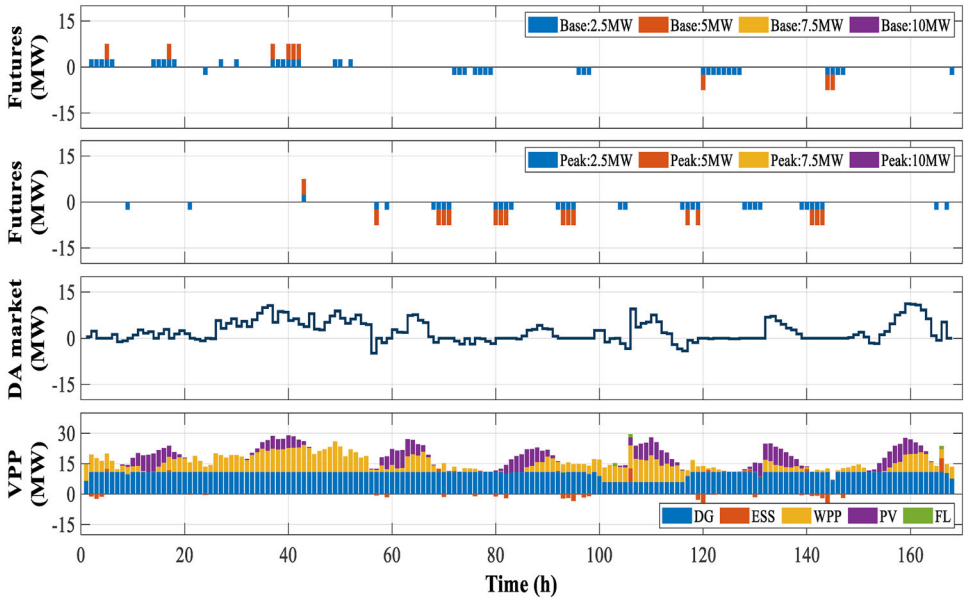

FIGURE 8 Generation of VPP and its interaction with DA and futures markets in case 3 with $\beta = 0$. DA, day-ahead; VPP, virtual power plant.

reducing the risk of problem, the expected profit of VPP can be decreased.

5.2.3 | Case 3

In case 2, VPP utilizes DG units during the week due to the low operating cost and high flexibility. However, these units may fail during the weekly timeframe of the problem. Therefore, it is necessary to consider the impact of DG unit failure, which is discussed in this case.

In case 3, different scenarios are generated to model the failure of DG units using the exponential distribution function [7]. First, 1000 scenarios are generated for each DG unit, and the generated scenarios are reduced to 10 using the widely used K-means method. The scenario generation and reduction process is repeated 10 times in order to ensure adequate coverage of the various DG unit failure scenarios. Therefore, 10 sets of 10 scenarios are obtained for each DG unit. The resulting scenarios are then merged and reduced to 15 final scenarios. Then, these scenarios are mixed with the scenarios of the previous case, and a total of $15 \times 45 = 675$ scenarios are obtained for case 3.

Due to considering the failure of DG units, the expected profit of VPP, in this case, is 728.099×10^3 €, which shows a reduction compared to the risk-neutral mode of the previous case. Like the previous case, the most probable scenarios are reported as the output of the problem. The generation power of VPP and its interaction with the DA and futures markets with $\beta = 0$ is presented in Figure 8. According to this figure, the interaction of VPP with the base contract is decreased, and VPP often appears as a buyer in the futures market. Moreover, the amount of exchanged power between VPP and the DA market is decreased compared to risk-neutral mode of the previous case. For example, in hours 101 to 116, when the second unit of DG is failed, the amount of sold power to the DA market is decreased. In this case, ESS are used more to compensate the lost power resulting from the failure of DG unit. It should be noted that due to the failure of DG unit, the power generation of VPP is reduced compared to risk-neural mode of the previous case.

Two factors of high fluctuations of the DA market price and the failure of DG units can increase the risk of problem in this case. Although the risk management can reduce the risk of problem due to these two factors, the expected profit of VPP can be also reduced. The risk-averse problem is solved in this case, and the expected profit of VPP is equal to 636.047×10^3 €, whereas the CVaR is equal to 605.579×10^3 €. Figure 9 illustrates the power generation of VPP and its interaction with the DA and futures markets with $\beta = 1$. It is shown that the amount of purchased power from the futures market is increased to compensate the lost power due to DG unit failure and to reduce risk. In addition, the amount of sold power to the DA market is decreased due to high price fluctuations. The amount of power generated by the DG unit is significantly reduced to decline the risk of problem. Therefore, the utilization of ESS is increased in this case.

5.2.4 | Case 4

The VPP participation in the DA and futures markets allows VPP to benefit from the price difference between these two markets when VPP acts as an arbitrageur. For example, when a VPP purchases power from the upstream network, it is probable to purchase surplus power from one market in order to sell the remained power at a higher price to another market. The constraints in (9)–(47) are used to solve this case ignoring the constraints in (26)–(28). By considering the failure of DG units,

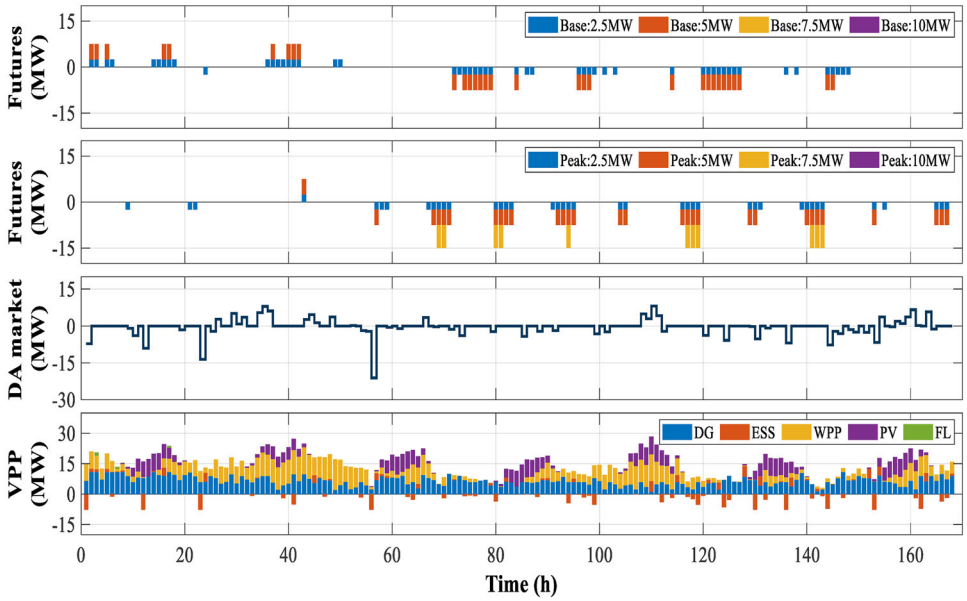

FIGURE 9 Generation of VPP and its interaction with DA and futures markets in case 3 with $\beta = 1$. DA, day-ahead; VPP, virtual power plant.

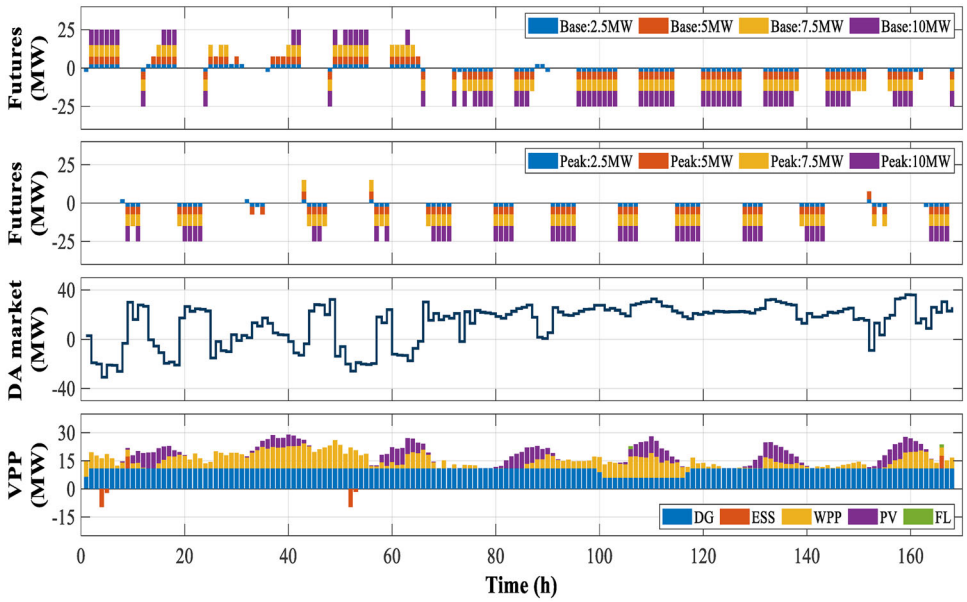

FIGURE 10 Generation of VPP and its interaction with DA and futures markets in case 4 with $\beta = 0$. DA, day-ahead; VPP, virtual power plant.

the expected profit of VPP, in case 4, is 828.753×10^3 €, which is higher than the expected profit of VPP in case 2. This comparison shows the importance of considering the advantage of an arbitrage opportunity. The power generation of VPP and its interaction with the DA and futures markets with $\beta = 0$ is presented in Figure 10. According to this figure, the exchanged power with the DA and futures markets is increased. Moreover, VPP exchanges more power than its consumption in these markets. For example, at hour 69, VPP needs to buy power from the upstream network to supply its loads. Therefore, due to the low price of the peak contract in the futures market, VPP buys surplus power from this market and sells the remained power to the DA market with a higher price. On the other hand, at hour 41, the amount of VPP power generation is more than its consumption. Therefore, VPP sells its extra power along with the purchased power from the DA market to the futures market to maximize the profit. As shown in Figure 10, VPP benefits from the exchange of power with the DA and futures markets, even when the second DG unit is failed (hours 101 to 116), which confirms the importance of arbitrage. Moreover, according to the obtained results presented in Figure 10, VPP often appears as a power seller in the DA market, which indicates the higher price of this market in comparison with the futures market.

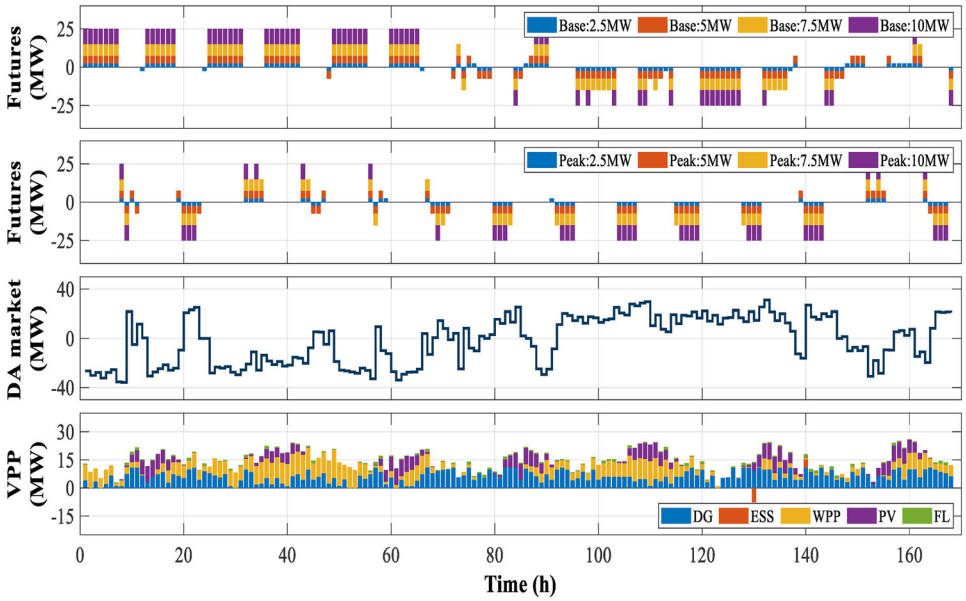

FIGURE 11 Generation of VPP and its interaction with DA and futures markets in case 4 with $\beta = 1$. DA, day-ahead; VPP, virtual power plant.

TABLE 4 Numerical results of the proposed VPP optimal bidding strategy problem for cases 2 to 4 in risk-neutral and risk-averse modes.

Results	Case 2		Case 3		Case 4	
	$\beta = 0$	$\beta = 1$	$\beta = 0$	$\beta = 1$	$\beta = 0$	$\beta = 1$
Expected profit ($\times 10^3$ €)	810.203	771.503	728.099	636.047	828.753	703.999
CVaR ($\times 10^3$ €)	755.113	771.128	387.328	605.579	427.202	666.547
Base contract revenue ($\times 10^3$ €)	26.472	48.918	1.419	−23.241	−186.225	81.421
Peak contract revenue ($\times 10^3$ €)	−22.475	−3.702	−35.529	−76.090	−300.545	−142.416
DX revenue ($\times 10^3$ €)	3.997	45.215	−34.110	−99.332	−486.770	−60.994
DA revenue ($\times 10^3$ €)	97.877	22.449	43.142	−10.835	601.916	45.124
Retail revenue ($\times 10^3$ €)	756.751	748.503	757.879	773.491	752.723	747.337
DGs cost ($\times 10^3$ €)	48.379	44.622	38.743	27.060	39.070	27.440
ESS cost ($\times 10^3$ €)	0.0434	0.0431	0.0684	0.214	0.0444	0.0278
DER cost ($\times 10^3$ €)	48.422	44.665	38.812	27.275	39.115	27.468

Abbreviations: CVaR, conditional value at risk; DX, Derivatives Exchange; DA, day-ahead; DER, distributed energy resource; DG, distributed generation; ESS, energy storage system; VPP, virtual power plant.

By solving the risk-averse problem, the expected profit of VPP is equal to 703.999×10^3 €, and the amount of CVaR is equal to 666.547×10^3 €. Figure 11 illustrates the power generation of VPP and its interaction with the DA and futures markets with $\beta = 1$. According to Figure 11, and similar to the risk-averse mode of case 3, VPP reduces its exchanged power with the DA market as well as the power generation of DG units to manage the problem risk. However, compared to the risk-averse mode of case 3, the expected profit of VPP is compensated to an acceptable level due to the arbitrage opportunity.

Table 4 summarizes the VPP revenues and costs in cases 2 to 4 with $\beta = 0$ and $\beta = 1$. As seen in this table, one of the primary sources of VPP's profit is the retail revenue, which is due to the high retail price. In other words, the high retail price encourages the VPP to supply its electrical loads first. This acknowledges that for the VPP operator, supplying electrical loads has a higher priority than participating in upstream markets. Another point that can be observed in Table 4 is the gap between the values of expected profit and CVaR when beta equals 1. The two main factors that increase the risk of the problem are DA market price scenarios and DG failure status scenarios. As shown in Figure 5, DA market price scenarios have a high variation range. In other words, the standard deviation of these scenarios is high. On the other hand, the failure status scenarios of DGs cover a wide range of statuses of these units. Additionally, since DGs are one of the main units of the VPP for power supply, their failure significantly impacts the VPP's profit. These factors increase the variation range of the objective

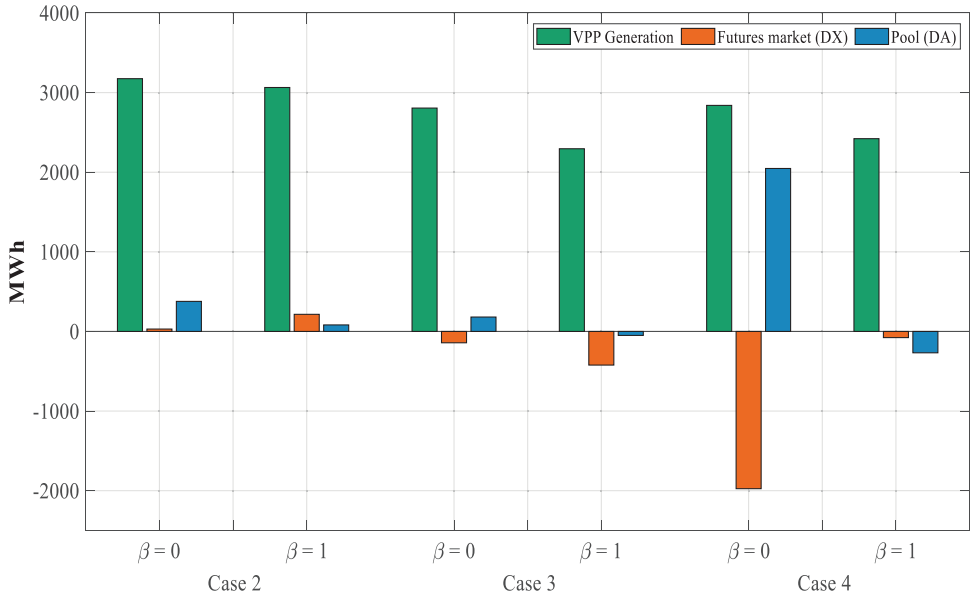

FIGURE 12 Expected power generation of VPP and its interaction with DA and futures markets in cases 2 to 4 for risk-neutral and risk-averse modes. DA, day-ahead; DX, Derivatives Exchange; VPP, virtual power plant.

function, and as a result, the gap between expected profit and CVaR increases. In addition, Figure 12 compares both risk-neutral and risk-averse results of the expected power generation of VPP and its interaction with DA and futures markets in all defined cases. According to this figure, for all cases, the exchange of VPP with the DA market is reduced by considering $\beta = 1$. It should be noted that the highest exchange with the markets is related to the risk-neutral mode of case 4, in which VPP uses the opportunity of arbitrage to increase its profit. Furthermore, the revenue obtained from the DA market in the risk-averse mode of case 4 is positive, even though the amount of power exchanged is negative. This indicates that although VPP often appears as a buyer in the DA market, it benefits from DA market during hours when the market price is high. It is important to note that using the opportunity of arbitrage is confirmed to be an effective solution for increasing the VPP's profit in the DA market.

6 | CONCLUSION

Here, the medium-term problem of the optimal bidding strategy of a technical and commercial VPP was modelled considering the risk constraints. The proposed VPP can participate in the DA and futures markets to maximize its profits. The impact of DG unit failure, which is the most widely used unit of VPP, was also examined in the proposed model. Many uncertainty parameters were considered in the proposed model, which first were predicted using the LSTM network with an acceptable accuracy, and then different scenarios were generated to cover their uncertainty.

The behaviour of VPP was examined in risk-neutral and risk-averse modes in each of the four considered cases. In case 1, a deterministic model of the problem was solved using actual and forecasted data to assess the accuracy of the LSTM network. The obtained results of case 1 confirmed that the LSTM network could accurately predict the uncertainty parameters. In case 2, the deterministic case is developed as a stochastic model ignoring the impact of DG units' failure. In a risk-neutral mode, regardless of the high price fluctuations in the DA market, VPP exchanged power with the upstream network. In the considered risk-averse mode, VPP reduced its interaction with the DA market and increased its interaction with the futures market. It is due to taking into account the high price fluctuations in the DA market. In case 3, the impact of DG units' failure was considered. The results of case 3 showed that the expected profit of VPP in the risk-neutral mode was decreased by 10.13% compared to the risk-neutral mode of case 2. In this case, the DA market price fluctuations and the failure of DG units were two factors that increased the risk. Therefore, in the risk-averse mode, although ESS utilization was increased, the interaction between VPP and the DA market along with the power generation of DG units were decreased. In case 4, the effect of using arbitrage opportunity was investigated. The results of this case showed that despite the DG units' failure impact, the expected profit of VPP increased by 13.82% compared to case 3, which confirmed the importance of being an arbitrageur. In summary, the results of this paper showed that the participation of the VPP in the futures market reduces the risk caused by the DA market prices and the DG units' failure. The participation of the VPP in both DA and futures markets also provides the possibility of using the arbitrage opportunity.

Although the LSTM neural network has an excellent ability to predict time series, it consumes a lot of memory and time in the learning process. As a result, other neural networks, such as gated recurrent unit, can be used to solve this issue.

Furthermore, other futures market contracts, such as call-option and put-option, can be implemented in this problem, which will be the subjects of future research.

NOMENCLATURE

Indices

b, b'	Indices of power blocks in futures market contracts
c, c'	Indices of futures market contracts
dg	Index of distributed generation (DG) units
ess	Index of energy storage systems (ESS)
fl	Index of flexible loads (FL)
i, j	Index of network nodes
k	Index of power blocks of DG units
pv	Index of photovoltaic (PV) units
s	Index of scenarios
t	Index of time periods (hour)
wpp	Index of wind power plant (WPP) units

Sets

Ω_B	Set of power blocks in futures market contracts
Ω_C	Set of futures market contracts
Ω_{DG}	Set of DG units in virtual power plant (VPP)
Ω_{ESS}	Set of ESS units in VPP
Ω_{FL}	Set of FL units in VPP
Ω_I	Set of network nodes
Ω_K	Set of power blocks of DG units
Ω_{PV}	Set of PV units in VPP
Ω_S	Set of scenarios
Ω_T	Set of time periods
Ω_{WPP}	Set of WPP units in VPP

Constants & Parameters

$\{\cdot\}^{min}$, $\{\cdot\}^{max}$	Minimum/maximum limits of bounded variables
S^{base}	Base apparent power (kVA)
λ^{Retail}	Retail price in distribution network (€/MWh)
Δt	Duration of each time period
α, β	Confidence level and weighting factor in conditional value at risk (CVaR) method
$B^{line}_{i,j}$	Susceptance of distribution line between node i and j (per unit)
DOD_{ess}	Depth of discharge of ESS units
$Load_{i,t,s}$	Electrical load of VPP in node i, period t, and scenario s (MW)
$P^{DX,Block}_{c,b}$	Maximum power can be sold/bought through the block b of futures market contract c (MW)
RU_{dg}, RD_{dg}	Ramp up/down of DG units (MW/h)
$TC^{DX}_{c,t}$	Connectivity matrix of allowed hours for trading in the futures market contract c
$UA_{dg,t,s}$	Connectivity matrix of availability of DG units (1 means DG unit is available and 0 means failure)
$a_{dg,k}$	Cost of DG units for block k (€/MWh)
a_{ess}	Degradation cost of ESS units (€/MWh)
η^{dch}_{ess}, η^{ch}_{ess}	Discharging/charging efficiency of ESS units
$\lambda^{DX,sell}_{c,b}$, $\lambda^{DX,buy}_{c,b}$	Selling/buying price of block b of futures market contract c (€/MWh)
$\lambda^{DA}_{t,s}$	Day-ahead (DA) market price in period t and scenario s (€/MWh)
π_s	Probability of occurrence of scenarios s

Variables

$PD_{i,t,s}$	Electrical demand in node i, in period t, and scenario s (MW)
$P^{DX,sell}_{c,b,t}$, $P^{DX,buy}_{c,b,t}$	Power sold/bought through the block k of futures market contract c (MW)
$P_{dg,t,s,k}$	Output power of block k of DG units in period t, and scenario s (MW)
$P^{i}_{dg,t,s}$	Total output power of DG units in node i, period t, and scenario s (MW)
$P^{dch}_{ess,t,s}$, $P^{ch}_{ess,t,s}$	Discharging/charging power of ESS units in period t, and scenario s (MW)
$P^{i}_{ess,t,s}$	Output power of ESS units in node i, period t, and scenario s (MW)
$P^{i}_{fl,t,s}$	Power curtailed by FL units in node i, period t, and scenario s (MW)
$P^{i}_{pv,t,s}$	Output power of PV units in node i, period t, and scenario s (MW)
$P^{DA,sell}_{t,s}$, $P^{DA,buy}_{t,s}$	Power sold/bought in the DA market (MW)
$P^{i}_{wpp,t,s}$	Output power of WPP units in node i, period t, and scenario s (MW)
$SOC_{ess,t,s}$	State of charge of ESS units in period t, and scenario s (MWh)
$flow_{i,j,t,s}$	Power flow between node i and j, in period t, and scenario s (MW)
$\delta_{i,t,s}$	Angle of node i, in period t, and scenario s
ξ	Value at risk (VaR)
η_s	Difference between VaR and profit of VPP in scenario s

Binary variables

$u^{DX,sell}_{c,b,t}$, $u^{DX,buy}_{c,b,t}$	Sign state of block b of futures market contract c in period t (1 means signed and 0 means not signed)
$u_{dg,t,s}$	On/off state of DG units
$u^{dch}_{ess,t,s}$, $u^{ch}_{ess,t,s}$	Discharging/charging state of ESS units
$u^{DA,sell}_{t,s}$, $u^{DA,buy}_{t,s}$	Sold/purchased power state of VPP in DA market.

AUTHOR CONTRIBUTIONS

Farzin Ghasemi Olanlari: conceptualization, methodology, validation, software, and writing—original draft preparation. Mojtaba Moradi-Sepahvand: supervision, validation, writing—reviewing and editing. Turaj Amraee: conceptualization, supervision, methodology, validation, and writing—reviewing and editing.

CONFLICT OF INTEREST STATEMENT

The authors have no conflicts of interest to declare. All co-authors agree with the contents of the manuscript and there is no financial interest to report. We certify that the submission is original work and is not under review at any other publication.

DATA AVAILABILITY STATEMENT

The data that support the findings of this study are available from the corresponding author upon reasonable request.

ORCID

Mojtaba Moradi-Sepahvand https://orcid.org/0000-0002-6531-1665
Turaj Amraee https://orcid.org/0000-0002-5198-0067

REFERENCES

1. Pérez-Arriaga, I.J.: In: Regulation of the Power Sector, p. 61. Springer, New York (2013)
2. Annual Energy Outlook 2022—U.S. Energy Information Administration (EIA). https://www.eia.gov/outlooks/aeo/. Accessed April 2022.
3. Mehigan, L., Deane, J.P., Gallachóir, B.P.Ó., Bertsch, V.: A review of the role of distributed generation (DG) in future electricity systems. Energy 163, 822–836 (2018)
4. Nosratabadi, S.M., Hooshmand, R.A., Gholipour, E.: A comprehensive review on microgrid and virtual power plant concepts employed for distributed energy resources scheduling in power systems. Renew. Sustain. Energy Rev. 67, 341–363 (2017)
5. Zhang, G., Jiang, C., Wang, X.: Comprehensive review on structure and operation of virtual power plant in electrical system. IET Gener. Transm. Distrib. 13(2), 145–156 (2019)
6. Garcés, L.P., Conejo, A.J.: Weekly self-scheduling, forward contracting, and offering strategy for a producer. IEEE Trans. Power Syst. 25(2), 657–666 (2010)
7. Pineda, S., Conejo, A.J., Carrión, M.: Impact of unit failure on forward contracting. IEEE Trans. Power Syst. 23(4), 1768–1775 (2008)
8. Arslan, O., Karasan, O.E.: Cost and emission impacts of virtual power plant formation in plug-in hybrid electric vehicle penetrated networks. Energy 60, 116–124 (2013)
9. Shahkoomahalli, A., Koochaki, A., Shayanfar, H.: Risk-based electrical-thermal scheduling of a large-scale virtual power plant using downside risk constraints for participating in energy and reserve markets. Arab. J. Sci. Eng. 47, 2663–2683 (2022)
10. Cui, H., Li, F., Hu, Q., Bai, L., Fang, X.: Day-ahead coordinated operation of utility-scale electricity and natural gas networks considering demand response based virtual power plants. Appl. Energy 176, 183–195 (2016)
11. Yang, Q., Wang, H., Wang, T., Zhang, S., Wu, X., Wang, H.: Blockchain-based decentralized energy management platform for residential distributed energy resources in a virtual power plant. Appl. Energy 294, 117026 (2021)
12. Gougheri, S.S., Jahangir, H., Golkar, M.A., Ahmadian, A., Aliakbar Golkar, M.: Optimal participation of a virtual power plant in electricity market considering renewable energy: a deep learning-based approach. Sustain. Energy, Grids Networks 26, 100448 (2021)
13. Hadayeghparast, S., SoltaniNejad Farsangi, A., Shayanfar, H.: Day-ahead stochastic multi-objective economic/emission operational scheduling of a large scale virtual power plant. Energy 172, 630–646 (2019)
14. Naval, N., Yusta, J.M.: Virtual power plant models and electricity markets - a review. Renew. Sustain. Energy Rev. 149, 111393 (2021)
15. Rahimi, M., Ardakani, F.J., Ardakani, A.J.: Optimal stochastic scheduling of electrical and thermal renewable and non-renewable resources in virtual power plant. Int. J. Electr. Power Energy Syst. 127, 106658 (2021)
16. Rashidizadeh-Kermani, H., Vahedipour-Dahraie, M., Shafie-khah, M., Siano, P.: A stochastic short-term scheduling of virtual power plants with electric vehicles under competitive markets. Int. J. Electr. Power Energy Syst. 124, 106343 (2021)
17. Vahedipour-Dahraie, M., Rashidizadeh-Kermani, H., Shafie-Khah, M., Catalão, J.P.S.: Risk-averse optimal energy and reserve scheduling for virtual power plants incorporating demand response programs. IEEE Trans. Smart Grid 12(2), 1405–1415 (2021)
18. Shabanzadeh, M., Sheikh-El-Eslami, M.K., Haghifam, M.R.: A medium-term coalition-forming model of heterogeneous DERs for a commercial virtual power plant. Appl. Energy 169, 663–681 (2016)
19. Jafari, M., Akbari Foroud, A.: A medium/long-term auction-based coalition-forming model for a virtual power plant based on stochastic programming. Int. J. Electr. Power Energy Syst. 118(September 2019), 105784 (2020)
20. Conejo, A.J., Carrión, M., Morales, J.M.: Futures market trading for producers. Int. Ser. Oper. Res. Manag. Sci. 153, 253–285 (2010)
21. Rezaee Jordehi, A.: A stochastic model for participation of virtual power plants in futures markets, pool markets and contracts with withdrawal penalty. J. Energy Storage 50(February), 104334 (2022)
22. Tan, Z., Fan, W., Li, H., et al.: Dispatching optimization model of gas-electricity virtual power plant considering uncertainty based on robust stochastic optimization theory. J. Clean. Prod. 247, 119106 (2020)
23. Rabiee, A., Sadeghi, M., Aghaeic, J., Heidari, A.: Optimal operation of microgrids through simultaneous scheduling of electrical vehicles and responsive loads considering wind and PV units uncertainties. Renewable Sustainable Energy Rev. 57, 721–739 (2016)
24. Sheidaei, F., Ahmarinejad, A.: Multi-stage stochastic framework for energy management of virtual power plants considering electric vehicles and demand response programs. Int. J. Electr. Power Energy Syst. 120, 106047 (2020)
25. Naghdalian, S., Amraee, T., Kamali, S., Capitanescu, F.: Stochastic network-constrained unit commitment to determine flexible ramp reserve for handling wind power and demand uncertainties. IEEE Trans. Ind. Informatics 16(7), 4580–4591 (2020)
26. Lekvan, A.A., Habibifar, R., Moradi, M., Khoshjahan, M., Nojavan, S., Jermsittiparsert, K.: Robust optimization of renewable-based multi-energy micro-grid integrated with flexible energy conversion and storage devices. Sustain. Cities Soc. 64, 102532 (2021)
27. Understanding LSTM Networks. http://colah.github.io/posts/2015-08-Understanding-LSTMs/. Accessed May 2022.
28. Brownlee, J.: Long Short-Term Memory Networks With Python Develop Sequence Prediction Models With Deep Learning. Machine Learning Mastery (2020)
29. Brownlee, J.: Deep Learning for Time Series Forecasting: Predict the Future with MLPs, CNNs and LSTMs in Python. Machine Learning Mastery (2018)
30. Ghasemi Olanlari, F., Amraee, T., Moradi-Sepahvand, M., Ahmadian, A.: Coordinated multi-objective scheduling of a multi-energy virtual power plant considering storages and demand response. IET Gener. Transm. Distrib. 16(17), 3539–3562 (2022)
31. Noorollahi, Y., Golshanfard, A., Hashemi-Dezaki, H.: A scenario-based approach for optimal operation of energy hub under different schemes and structures. Energy 251, 123740 (2022)
32. Conejo, A.J., Carrión, M., Morales, J.M.: Decision Making Under Uncertainty in Electricity Markets. Springer US, New York (2010)
33. Conejo, A.J., García-Bertrand, R., Carrión, M., Caballero, Á., de Andrés, A.: Optimal involvement in futures markets of a power producer. IEEE Trans. Power Syst. 23(2), 703–711 (2008)
34. ENTSO-E: ENTSO-E transparency Platform. Entso-E 1–20 (2018). https://transparency.entsoe.eu/ May 2022

35. OMIP: https://www.omip.pt/en/. Accessed April 2022.
36. Institute National Wind: West Texas Mesonet. http://rain.ttu.edu/tech/1-output/current.php. Accessed April 2022.
37. Premono, B.S., Tjahjana, D.D.D.P., Hadi, S.: Wind energy potential assessment to estimate performance of selected wind turbine in northern coastal region of Semarang-Indonesia. In: AIP Conference Proceedings, p. 030026. AIP Publishing LLC, New York (2017)
38. Latreche, Y., Bouchekara, H.R.E.H.: Comprehensive review of radial distribution test systems. *TechRxiv*, **Preprint**, pp. 1–65 (2020)
39. Lima, R.M., Novais, A.Q., Conejo, A.J.: Weekly self-scheduling, forward contracting, and pool involvement for an electricity producer. An adaptive robust optimization approach. Eur. J. Oper. Res. 240(2), 457–475 (2015)
40. Derivatives | OMIP. https://www.omip.pt/en/dados-mercado/. Accessed April 2022.
41. Electricity price statistics - Statistics Explained. https://ec.europa.eu/eurostat/statistics-explained/index.php?title=Electricity_price_statistics. Accessed May 2022.
42. IEEE reliability test system: A report prepared by the Reliability Test System Task Force of the Application of Probability Methods Subcommittee. IEEE Trans. Power Appar. Syst. PAS-98(6), 2047–2054 (1979)
43. Python Software Foundation: Welcome to Python.org. https://www.python.org/about/. Accessed April 2022.
44. Keras: the Python deep learning API. https://keras.io/. Accessed April 2022.
45. TensorFlow. https://www.tensorflow.org/. Accessed April 2022.
46. Kingma, D.P., Ba, J.L.: Adam: a method for stochastic optimization. In: Proceedings of the 3rd International Conference on Learning Representations, ICLR 2015. (2015)
47. GAMS Development Corp.: GAMS - Cutting edge modeling. (2021). https://www.gams.com/
48. ILOG CPLEX Optimization Studio | IBM. https://www.ibm.com/products/ilog-cplex-optimization-studio. Accessed April 2022.
49. Kazemzadeh, M.R., Amjadian, A., Amraee, T.: A hybrid data mining driven algorithm for long term electric peak load and energy demand forecasting. Energy 204, 117948 (2020)

How to cite this article: Ghasemi-Olanlari, F., Moradi-Sepahvand, M., Amraee, T.: Two-stage risk-constrained stochastic optimal bidding strategy of virtual power plant considering distributed generation outage. IET Gener. Transm. Distrib. 1–18 (2023). https://doi.org/10.1049/gtd2.12826